

Comprehensive Molecular Characterization of Atmospheric Brown Carbon by High Resolution Mass Spectrometry with Electrospray and Atmospheric Pressure Photoionization

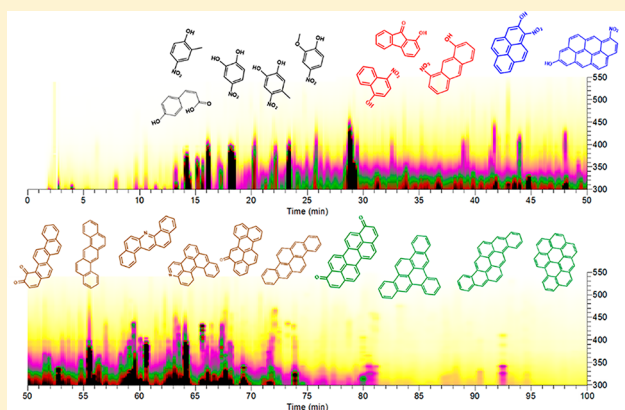
Peng Lin,[†] Lauren T. Fleming,[‡] Sergey A. Nizkorodov,[‡] Julia Laskin,[†] and Alexander Laskin^{*,†}

[†]Department of Chemistry, Purdue University, West Lafayette, Indiana 47907-2084, United States

[‡]Department of Chemistry, University of California, Irvine, California 92697-2025, United States

Supporting Information

ABSTRACT: Light-absorbing components of atmospheric organic aerosols, which are collectively termed “brown carbon” (BrC), are ubiquitous in the atmosphere. They affect absorption of solar radiation by aerosols in the atmosphere and human health as some of them have been identified as potential toxins. Understanding the sources, formation, atmospheric evolution, and environmental effects of BrC requires molecular identification and characterization of light-absorption properties of BrC chromophores. Identification of BrC components is challenging due to the complexity of atmospheric aerosols. In this study, we employ two complementary ionization techniques, atmospheric pressure photo ionization (APPI) and electrospray ionization (ESI), to obtain broad coverage of both polar and nonpolar BrC components using high-resolution mass spectrometry (HRMS). These techniques are combined with chromatographic separation of BrC compounds with high performance liquid chromatography (HPLC), characterization of their light absorption with a photodiode array (PDA) detector, and chemical composition with HRMS. We demonstrate that this approach enables more comprehensive characterization of BrC in biomass burning organic aerosols (BBOAs) emitted from test burns of sage brush biofuel. In particular, we found that nonpolar BrC chromophores such as PAHs are only detected using positive mode APPI. Meanwhile, negative mode ESI results in detection of polar compounds such as nitroaromatics, aromatic acids, and phenols. For the BrC material examined in this study, over 40% of the solvent-extractable BrC light absorption is attributed to water insoluble, nonpolar to semipolar compounds such as PAHs and their derivatives, which require APPI for their identification. In contrast, the polar, water-soluble BrC compounds, which are detected in ESI, account for less than 30% of light absorption by BrC.



Biomass burning (BB) in the form of wildfires, prescribed fires, or domestic biofuel burning releases a large amount of smoke particles contributing significantly to the overall atmospheric organic aerosol (OA).¹ BB smoke particles affect visibility and air quality,² cause adverse health effects,³ act as ice and cloud condensation nuclei,⁴ and contribute to Earth's radiative forcing ultimately affecting climate.^{5,6} The extent of these effects strongly depends on the physical properties and chemical composition of BB aerosols, which are still insufficiently understood. The lack of fundamental knowledge about BB composition and properties results in large uncertainties in modeling BB's impact.⁷

BB smoke particles contain complex mixtures of black carbon (BC), organic carbon (OC), inorganic salts, and oxides that all have critical air quality and climate impacts. Light absorption properties of these mixtures are of particular interest to this paper. Radiative forcing by BC due to light absorption and scattering has been extensively studied; BC emissions inventories and optical properties have been

incorporated into climate models.⁸ However, there is still substantial discrepancy between model predictions and surface- or satellite-based observations of the aerosol optical density.^{9,10} This gap is attributed in part to poor description of the OC compounds strongly absorbing solar radiation in the near-UV and visible regions in the models.¹¹ This class of OC is collectively termed “brown carbon” (BrC) due to its characteristic yellow to brown color appearance and the absorption spectrum with strong wavelength dependence.¹²

Although BrC has been recognized as a significant contributor to light absorption,¹³ quantitative predictions of its atmospheric effects are still challenging because of its chemical complexity and high reactivity.^{14,15} All organic aerosols, including BrC, contain a large number of organic

Received: May 15, 2018

Accepted: October 8, 2018

Published: October 8, 2018

compounds with diverse molecular structures, a substantial fraction of which have not been identified yet.¹⁶ Numerous studies indicate that optical properties of BrC may significantly evolve as a result of atmospheric processes such as oxidation,^{17,18} solar irradiation,^{19,20} changes in temperature,²¹ and relative humidity.^{22–24} These factors make the chemical composition and concentration of BrC chromophores highly variable across sources and locations.^{14,15} Because light absorption properties of organic compounds strongly depend on their structures,²⁵ detailed structural characterization of BrC compounds is essential to understanding their sources and transformation processes in the atmosphere.

Characterization of BrC composition and optical properties has been a subject of numerous studies over the past decade, and major findings have been summarized in multiple reviews.^{12,14,15,26} Many studies focused on evaluating light absorption of BrC by characterizing the properties of the water-soluble fraction of OC (WSOC). For example, online measurements of water-extractable BrC have been performed using a particle into liquid sampler coupled to an UV–vis spectrometer.^{27,28} This technique has been widely employed in field measurements to assess the contribution of WSOC to the total light absorption. Other studies focused on molecular speciation of WSOC and attempted to link light absorption to their chemical composition.^{29–31} The results suggested that nitro-aromatic compounds, particularly nitro-phenols, are abundant BrC chromophores in WSOC, and BB emissions are one of the most important BrC sources.^{32,33}

In addition, it has been demonstrated that BrC extracts in polar organic solvents, such as methanol or acetonitrile, usually are more absorbing than WSOC.^{34,35} These reports imply that a considerable fraction of light absorption may be attributed to the water-insoluble fraction of OC (WIOC).³⁶ Moreover, analysis of BrC extracts in a nonpolar hexane solvent showed that light absorption by the nonpolar water-insoluble fraction of OC in BB emissions is comparable or even higher than that of WSOC.^{37,38} Chemical composition of the nonpolar OC constituents has been traditionally investigated using gas chromatography/mass spectrometry (GC/MS).^{39,40} However, their light absorption properties are rarely measured. Although the GC-UV hyphenation has been developed for half century,⁴¹ its applications are mainly in the UV⁴² and vacuum UV range.⁴³ Our previous studies demonstrated that a combination of high performance liquid chromatography (HPLC), photodiode array (PDA) detector, and high-resolution mass spectrometry (HRMS) is a powerful platform for chemical characterization of BrC chromophores in OA.^{33,44} This technique separates solvent-extractable BrC compounds into fractions with characteristic retention times, UV–vis absorption spectra, and elemental⁴² composition offering useful insights into their plausible molecular structures.^{45,46} Similar techniques were employed to separate, identify, and quantify BrC chromophores in cloudwater,³² ambient aerosols,^{30,47} and biomass burning smoke particles.⁴⁸ All these studies used electrospray ionization (ESI) to generate molecular ions for MS measurement. While ESI is a soft ionization method, it can only ionize polar organic compounds. In particular, nonpolar or less polar compounds such as polycyclic aromatic hydrocarbons (PAHs) and saturated hydrocarbons are not easily ionized by ESI. This is of particular concern when analyzing BrC because they are expected to contain PAHs.⁴⁹ For example, our previous study of BrC in BB smoke particles suggested that a significant

portion of light absorption by biomass burning organic aerosol (BBOA) originates from PAH derivatives, such as oxo-PAHs,⁴⁴ which suggests that unsubstituted PAHs may also be present in the mixtures. Therefore, a combination of different ionization methods is needed to observe both polar and nonpolar compounds in BrC.

Atmospheric pressure photoionization (APPI) and chemical ionization (APCI) are appropriate alternatives for ionization of less polar compounds, which are not readily ionized by ESI. APPI is known to offer less ion suppression, wider dynamic range, and higher sensitivity to nonpolar compounds and especially PAHs compared with APCI and ESI.^{50,51} It has been demonstrated that APPI-HRMS is ideally suited for the analysis of PAHs in aerosol samples⁵² and condensed aromatic structures in marine dissolved organic matter.⁵³ In this study, we used both ESI and APPI as complementary ionization techniques, which allowed us to extend the analytical window of the BrC characterization to include its nonpolar constituents. Proof-of-concept experiments focused on chemical analysis of a sample of BB smoke particles from sage brush burning to demonstrate the utility of this approach for comprehensive chemical characterization of BrC in BBOA samples. We show that as much as 40% of the total absorbance in solvent-extractable BrC in sagebrush BBOA is attributable to nonpolar PAH molecules, which would not be detected with ESI-based methods. This work emphasizes the critical need to combine multiple ionization modes for a comprehensive description of BrC composition and light absorption properties. Extending the range of identified light-absorbing constituents to nonpolar species will therefore improve our predictive understanding of BrC sources and its composition, chemical transformations, and optical properties.

■ EXPERIMENTAL SECTION

BBOA samples were collected during the first intensive campaign of the Fire Influence on Regional and Global Environmental Experiment (FIREX) conducted at the U.S. Forest Service Fire Science Laboratory (FSL) in Missoula, MT, where a series of laboratory measurements and aerosol sampling of biomass burning emissions were performed in October and November of 2016. FIREX is a multiyear project targeting the critical unknowns about BB with an aim to better understand and predict the impact of North American fires on climate and air quality. Detailed description of FIREX and the FSL facility have been presented elsewhere.⁵⁴ During FIREX 2016, different biomass materials characteristic of the Western North America area as well as other types of biofuels of global importance were burned in the FSL facility. A full description of FIREX experiments including biomass collection location, elemental content, burning conditions, etc. is provided in a recently published paper;⁵⁴ additional information is available in the NOAA archive via <https://esrl.noaa.gov/csd/projects/firex/firelab/>. During the burning experiments, BBOA smoke particles were collected on polytetrafluoroethylene (PTFE) membrane filters (47 mm, Millipore Sigma) through a PM_{2.5} cyclone inlet operating at a flow rate of 16.7 L/min. The filter samples were sealed immediately at the end of each sampling task and stored at –18 °C pending analysis.

Portions of the aerosol-loaded filters were extracted with 5 mL of solvent in an ultrasonic bath for 40 min. Three different solvents were used: (1) ultrapure water, (2) acetonitrile, and (3) a mixture of three organic solvents with broad polarity hereafter referred to as “orgmix” (acetonitrile/dichlorome-

thane/hexane = 2:2:1 by volume). The extracts were filtered using syringe filters with 0.45 μm PTFE membrane to remove insoluble suspended particles. UV–vis absorption spectra of the resulting BrC solutions were acquired using an UV–vis spectrometer (USB 2000+, Ocean Optics) in a 1 cm quartz cuvette over a 250–900 nm wavelength range. Pure solvent served as a reference. The UV–vis spectroscopy measurement suggested that the “orgmix” generally yields the higher extraction efficiency for BrC compounds, compared to extraction by pure water and acetonitrile.³³ So, the “orgmix” extract was selected for further chemical characterization. 1.5 mL of the “orgmix” extract was preconcentrated to 0.5 mL and then mixed with 0.5 mL of methanol solution (containing 10% of H_2O) to make a final solution ready for direct infusion ESI-HRMS analysis. Another 1.5 mL of the “orgmix” extract was preconcentrated to 0.5 mL and then mixed with 0.5 mL of toluene to make a final solution ready for direct infusion APPI-HRMS analysis. The remaining ~ 2 mL of “orgmix” extract was preconcentrated and reconstituted in 200 μL of dimethyl sulfoxide (DMSO) to make a final solution ready for HPLC-PDA-ESI/APPI-HRMS analysis.

The direct infusion HRMS analysis experiments were performed via injecting the sample solution through a commercial atmospheric pressure ionization source (IonMAX API) at a flow rate of 5 $\mu\text{L}/\text{min}$ and measured directly with a high resolution LTQ-Orbitrap mass spectrometer (Thermo Electron, Inc.) operated with a resolving power of 100 000 at m/z 400. For ESI-HRMS analysis, a spray voltage of -2.5 and $+3$ kV was applied to the capillary in negative and positive ionization mode, respectively. For APPI-HRMS analysis, the APPI probe is equipped with a PhotoMate light source using a krypton lamp that emits photons with energies of 10.0 and 10.6 eV, capable of ionizing a wide range of less polar analytes.

Chemical speciation of BrC chromophores was analyzed using a HPLC-PDA-HRMS platform interfaced with either APPI or ESI ion sources. The platform consists of a Surveyor Plus system (including a quaternary LC pump, auto sampler, and PDA detector), an IonMAX ionization source that was configured as either ESI or APPI, and a high resolution LTQ-Orbitrap mass spectrometer (all modules are from Thermo Electron, Inc.). The separation was performed on a reverse-phase column (Luna C18, $2 \times 150 \text{ mm}^2$, 5 μm particles, 100 \AA pores, Phenomenex, Inc.). The binary solvent included: (A) water with 0.05% v/v formic acid and (B) ultrapure grade acetonitrile with 0.05% v/v formic acid. Gradient elution was performed by the A + B mixture at a flow rate of 200 $\mu\text{L}/\text{min}$: 0–3 min hold at 90% A, 3–62 min linear gradient to 10% A, 63–75 min hold at 10% A, 76–89 min linear gradient to 0% A, 90–100 min hold at 0% A, and then 101–120 min hold at 90% A to recondition the column for the next sample. The pH of the mobile phase was between 3 and 4 during the gradient period, measured with pH test strips (SIGMA P4661, 0.0–6.0 pH; resolution: 0.5 pH unit). UV–vis absorption spectra were measured using the PDA detector over the wavelength range of 200–700 nm. The ESI settings were as follows: 4.0 kV spray potential, 35 units of sheath gas flow, 10 units of auxiliary gas flow, and 8 units of sweep gas flow. The IonMAX dopant-assisted APPI source was employed to ionize compounds that are not readily ionized by the ESI source. Typical APPI settings are 400 $^\circ\text{C}$ vaporizer temperature, 50 units of sheath gas flow, 5 units of auxiliary gas flow, and 0 units of sweep gas flow. A mixture of 3-(trifluoromethyl)anisole (TFMA) and chlorobenzene (1:99 v/v) solution was used as a dopant to

promote proton transfer and charge exchange reactions necessary for the sensitive detection of a wide range of nonpolar compounds.⁵⁵ The dopant was delivered at 20 $\mu\text{L}/\text{min}$ using a syringe pump and combined with the mobile phase after exiting the column and before entering the ion source using a tee adaptor. Additional experiments were performed in the direct infusion mode, without the column. These experiments provided the overall absorption spectrum of the unseparated mixture recorded with a PDA.

Xcalibur (Thermo Scientific) software was used to acquire raw data. The HPLC-PDA-HRMS data were processed with an open source software toolbox, MZmine 2 (<http://mzmine.github.io/>), to perform peak deconvolution and chromatogram construction.⁵⁶ The differences of RTs between the signals recorded by HRMS and PDA detectors were corrected using standard compounds with known UV–vis spectra.⁴⁶ Analysis and assignments of MS peaks were performed using a suite of Microsoft Excel macros developed in our group.⁵⁷ The CH_2 -based first-order transformation was followed by the H_2 -based second-order transformation, which enabled clustering of the two-dimensional homologous series of peaks separated by the number of CH_2 and H_2 units into distinctive groups. Identification of one member in each group uniquely identifies all other members of the group. Our previous study demonstrated that this approach significantly reduces the complexity and simplifies the analysis of high-resolution mass spectra of complex mixtures.^{57,58} Elemental formulas of one representative peak from each group of homologous peaks were assigned using the MIDAS molecular formula calculator (<http://magnet.fsu.edu/~midas/>). Formula assignments were performed using the following constraints for the number of atoms in the ion: $\text{C} \leq 100$, $\text{H} \leq 200$, $\text{N} \leq 3$, $\text{O} \leq 50$, $\text{S} \leq 1$, and $\text{Na} \leq 1$. The double-bond equivalent (DBE) values of the neutral formulas were calculated using the following equation: $\text{DBE} = c - h/2 + n/2 + 1$, where c , h , o , n , and s correspond to the number of carbon, hydrogen, oxygen, nitrogen, and sulfur atoms in the neutral formula, respectively. The aromaticity index (AI)^{59,60} was calculated using the equation $\text{AI} = [1 + c - o - s - 0.5h]/(c - o - n - s)$.

RESULTS AND DISCUSSIONS

It has been demonstrated that HPLC-PDA-HRMS is a powerful method for the identification of BrC chromophores.^{33,44–46} In these experiments, BrC is extracted from the filter sample into a solvent, making the results dependent on the extraction solvent. To examine the effect of the extraction solvent on the solution composition, we compared UV–vis spectra of bulk BrC solutions extracted with three different solvents: orgmix, acetonitrile, and water as shown in Figure S1. Although the shapes of the absorption spectra are similar in all three solvents, the amount of BrC light absorption detected in the solvent extracts follows the trend of orgmix > acetonitrile > water. This result suggests that a significant portion of BrC light absorption is likely attributed to nonpolar and low-polarity compounds insoluble in water.

Solvent (orgmix) extracts of BBOA were first analyzed with direct infusion ESI/APPI-HRMS. To the best of our knowledge, APPI has not previously been used for molecular analysis of BBOA. Therefore, it was necessary to compare the results obtained by APPI-HRMS with the more widely used ESI-HRMS. Mass spectra acquired using ESI and APPI, each in positive ion and negative ion modes (hereinafter abbreviated as ESI+, ESI–, APPI+, and APPI–), are shown in Figure 1a,b.

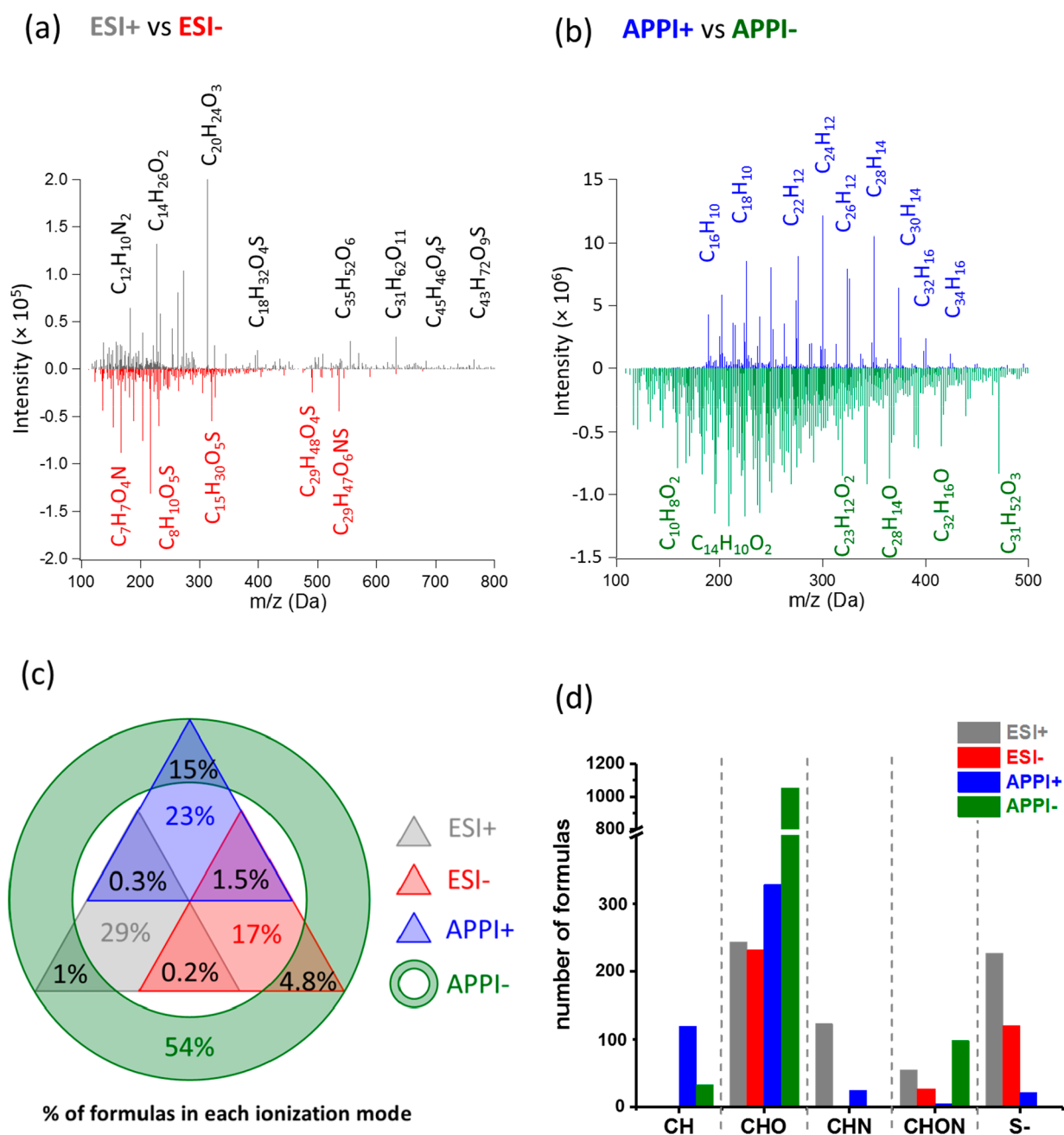


Figure 1. Mass spectra of solvent-extractable organic compounds measured with direct infusion ESI-HRMS (a) and APPI-HRMS (b), respectively. The mass spectra were acquired with both positive and negative charge modes. Molecular formulas correspond to neutral molecules. Number percentages of elemental formulas identified in each ionization mode (c); histogram of amount of elemental formulas of each of the listed heteroatom classes in BBOA, observed by ESI or APPI modes of measurements (d).

Very different mass spectra were obtained with these four modes of ionization. The ESI+ mass spectrum contains peaks corresponding to neutral compounds with molecular weights (MW) between 100 and 800 (Figure 1a). A significant amount (47%) of high molecular weight (HMW) compounds (MW > 500 Da) was detected with ESI+ mode. Compounds observed by the other three ionization modes are mainly within the range of $100 < MW < 500$ Da.

Overall, 2209 unique elemental formulas were identified in the mass spectra obtained with these four ionization methods. Out of them, only 29% and 17% were identified using ESI+ and ESI– mode, respectively (Figure 1c). A larger fraction of the observed compounds, 54% and 23% were detected in

APPI– and APPI+ modes. Moreover, the lists of elemental formulas identified in each of the modes are largely mutually exclusive with limited overlap between the species detected in different ionization modes. A side-by-side comparison of the molecular formulas detected in each mode suggests that only a small fraction of molecular compositions was observed in two different modes (Figure 1c). For example, only 0.2% of compounds were detected in both ESI+ and ESI– modes; 0.3% of compounds were detected in both APPI+ and ESI+ modes. Remarkably, not a single compound was detected by all four ionization modes. This result is attributed to the major differences in the ionization mechanisms: ESI selectively ionizes polar molecules that have acidic or basic functionalities

detected as ions with different polarities. In contrast, APPI ionizes nonpolar molecules through electron detachment or charge transfer between a photoionized dopant and other ions present within the sample. Therefore, this observation supports the argument that combined ESI and APPI analyses are necessary to provide a more complete molecular characterization of BBOA. The small degree of overlap between the compounds found in different ionization modes suggests that some of the BBOA compounds may still remain undetected. Even with the broader range of coverage afforded by the ESI/APPI combined data set, some of the compounds may escape detection if they do not ionize well in any of the four ionization methods used in this study. Another possible reason for this poor overlap between ESI and APPI could be that the ionization processes of APPI are more complicated than those of ESI. Protonated molecules, deprotonated molecules, and radical ions, as well as fragmentation and substitution products, are formed simultaneously in the APPI source,⁶¹ which complicated their spectra. However, the extent of ions formed through fragmentation and substitution has not been well evaluated yet, and more efforts are warranted to address this issue in the future.

The identified formulas are further classified into five major compound categories, including CH, CHO, CHN, CHON, and S (sulfur containing compounds), based on their elemental composition. CHON refers to compounds that contain carbon, hydrogen, oxygen, and nitrogen elements. Other compound categories are defined analogously. The S compounds include species with both CHOS (95% of S compounds) and CHONS (5%) composition. The numbers of formulas identified using different ionization techniques and compound categories are summarized in Figure 1d. CHO is the most abundant category observed by both APPI and ESI. APPI– detects an overwhelmingly large number of CHO compounds compared with other ionization modes. ESI is more efficient in ionizing S compounds. Most of the S compounds were selectively ionized by ESI–, suggesting that they are polar species such as organo-sulfates. CH compounds were only detected in APPI mass spectra, particularly in the positive ion mode. As shown in Figure 1b, the APPI+ mass spectrum is largely dominated by ions of CH compounds. Many of them are detected as ion-radicals with high values of $\text{DBE} \geq 12$ and $\text{AI} > 0.7$, indicative of PAHs with an extensive network of aromatic and conjugated carbon–carbon bonds.

Additional information about the molecular structures of compounds identified with these four ionization modes can be inferred from Figure 2, which shows a plot of DBE versus carbon number based on the assigned formulas. The data are shown along with the reference to DBE values characteristic of (a) linear polyenes with a general formula C_xH_{x+2} , characterized by $\text{DBE} = 0.5 \times c$; (b) *cata*-condensed PAHs,⁶² with $\text{DBE} = 0.75 \times c - 0.5$; (c) fullerene-like hydrocarbons with $\text{DBE} = 0.9 \times c$.⁶³ Since efficient absorption of visible light by an organic molecule requires uninterrupted conjugation across a significant part of the molecular skeleton, compounds with DBE/C ratio greater than that of polyenes are potential BrC chromophores. The shaded area in Figure 2 highlights the compounds that match this criterion. Remarkably, a majority (>96%) of the compounds detected with APPI are in this region. The deviation between DBE values observed in APPI and ESI modes is particularly pronounced for higher-MW compounds containing more than 25 carbon atoms, which may contain longer networks of conjugated and aromatic bonds

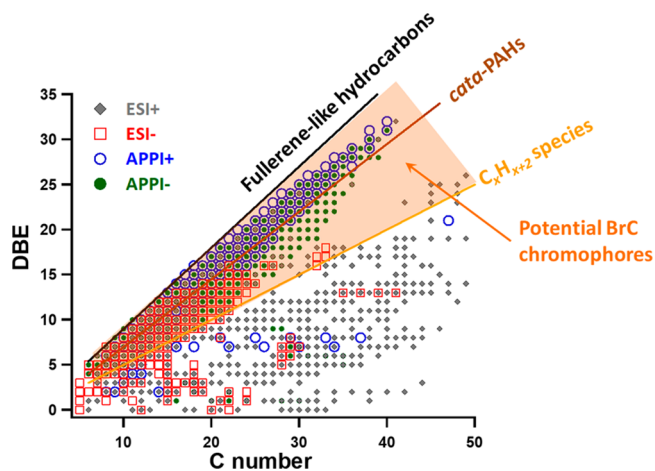


Figure 2. Plot of the double bond equivalent (DBE) vs number of carbon atoms in identified BBOA species detected in four ionization modes. Lines indicate DBE reference values of linear conjugated polyenes C_xH_{x+2} (yellow solid line), *cata*-condensed PAHs (brown solid line), and fullerene-like hydrocarbons with $\text{DBE} = 0.9 \times c$ (black solid line). Data points inside the orange shaded area are potential BrC chromophores (more details in the main text).

capable of stronger absorption in the visible range. Around 65% of compounds detected in ESI– mode are located in the “BrC domain” marked by the orange area. However, most of the ESI detected compounds are smaller molecules with fewer than 25 carbon atoms. For ESI+, only 24% of detected compounds are within the “BrC domain”, implying that ESI+ mode preferentially ionizes compounds in the BBOA sample with substantially more aliphatic carbon skeleton character.

The results in Figure 2 suggest that APPI efficiently ionizes species with relatively high DBE/C ratios, and more BrC chromophores are detected using APPI than ESI. Thus, APPI appears as a more suitable ionization source for BrC molecular analysis. This is partly true for the direct infusion ESI-HRMS and APPI-HRMS measurements, because matrix effects of the complex organic mixture may significantly affect the abundance of peaks corresponding to BrC chromophores. While it is suggested that APPI usually has little or no ion suppression, the suppression issue is very common to ESI due to competition for charge among individual analyte molecules.⁵³ As a result, later, we found that many abundant ions detected by direct infusion APPI+ mode HRMS analysis (e.g., $\text{C}_{18}\text{H}_{10}$, $\text{C}_{22}\text{H}_{12}$, $\text{C}_{24}\text{H}_{12}$, $\text{C}_{26}\text{H}_{12}$, $\text{C}_{28}\text{H}_{14}$, $\text{C}_{30}\text{H}_{14}$, etc. in Figure 1b) were also detected as the major BrC chromophores by the HPLC-PDA-HRMS method (Table S1). On the other hand, because of the matrix effect, many abundant ions detected by direct infusion ESI+ and ESI– HRMS analysis (e.g., sulfur containing compounds in Figure 1a) does not match the major BrC chromophores by the HPLC-PDA-HRMS method (Table S1).

Variability in ionization efficiency for individual compounds in ESI mode results in either selectively preferred or hindered ionization of organic compounds with certain molecular structures. This selectivity, combined with the complexity of BBOA analyte, makes it difficult to quantitatively assess mass spectra of BBOA obtained through direct infusion HRMS analysis. High or low peak abundance (relative intensity) is not a direct reflection of high or low analyte concentration, and therefore, quantitative comparison of MS data between different ionization methods is not straightforward.

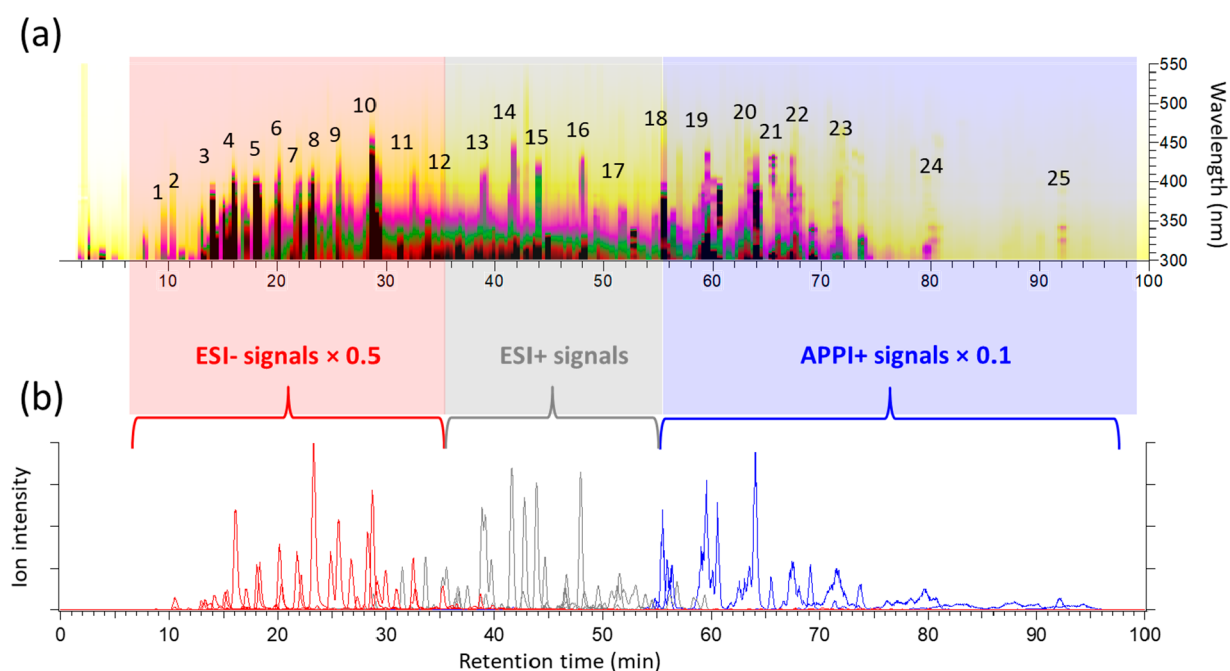


Figure 3. HPLC-PDA (a) and HPLC-HRMS (b) chromatograms of BBOA sample. The x -axis is HPLC retention time. The y -axis and color map in panel (a) refer to the wavelength and the UV-vis absorbance, respectively. The numbers on the color map denote 25 major light absorption peaks detected by PDA. Panel (b) shows a compilation of selected ion chromatograms (SIC) for the most abundant peaks detected with different modes of ionization (red for ESI $-$, gray for ESI $+$, and blue for APPI $+$). The APPI and ESI $-$ signals are decreased by factors of 10 and 2, respectively, for better visualization on the plots of panel (b). The retention times shown in panels (a) and (b) are corrected for the time delay (~ 0.4 min) between MS and PDA detectors.

In order to better identify the major BrC chromophores and more quantitatively evaluate their contribution to the overall BrC light absorption, the BBOA sample was further analyzed with the HPLC-PDA-HRMS methods. Similar to the direct infusion experiments, ionization in positive and negative ESI and APPI modes were employed in four separate HPLC-PDA-HRMS experiments with the same HPLC separation protocol, as described in the experimental section.

Figure 3a shows an HPLC-PDA chromatogram, where the x -axis corresponds to the retention time (RT), the y -axis shows the PDA wavelength, and the measured absorbance is encoded by the heatmap colors. The chromatogram shows a large number of well-separated chromophores eluting at different RTs between 10 and 100 min. A substantial fraction of their light absorption lies in the visible wavelength range of >400 nm. The chemical composition of these chromophores was investigated in four separate experiments using HRMS operated in positive and negative APPI and ESI modes.

The composition of specific BrC chromophores was identified by examining time periods of the HPLC-HRMS chromatograms corresponding to pronounced light absorption peaks observed in the HPLC-PDA chromatogram. We note that under current HPLC mobile-phase conditions (i.e., gradient elution by solvents with pH = 3), which were chosen to promote separation of BrC chromophores, the HPLC-APPI/HRMS chromatogram detects a substantially smaller number of ions than that detected by the direct infusion APPI/HRMS analysis (e.g., Table S1 and Appendix S1). One possible reason is that the HPLC method was only optimal for eluting PAHs < 300 Da,^{50,64} while some larger highly nonpolar compounds, such as PAHs and other condensed aromatic compounds with MW > 400 (e.g., C₃₂H₁₆ and C₃₄H₁₆ in Figure 1b) are probably insufficiently eluted from the column

under current HPLC conditions. Another more important reason is that the acidic mobile phase provides a protic environment that suppresses negative APPI processes, during which the negative ions are formed by proton transfer to form a deprotonated molecule, by electron capture, or by other charge exchange processes.⁶⁵ As a result, the HPLC-PDA-HRMS data discussed below relies mostly on the MS results acquired in ESI $-$, ESI $+$, and APPI $+$ modes.

Figure 3b shows a compilation of selected ion chromatograms (SIC) of the most abundant ions detected by different modes of ionization. BrC chromophores that eluted at RTs between 0 and 33 min showed strong MS signals detected in the ESI $-$ mode. BrC chromophores, which eluted between 33 and 55 min correlated well with MS signals detected in the ESI $+$ mode. Finally, BrC chromophores, which eluted after 55 min showed excellent correlation with MS data acquired in APPI $+$ mode. These observations are consistent with the retention behavior of organic molecules by the reverse-phase C18 column, where hydrophilic polar compounds (WSOC such as organic acids) elute faster while hydrophobic nonpolar species (WIOC such as PAHs and quinones) elute later due to their stronger interactions with the stationary phase.

For the BrC chromophores observed in both the PDA and MS chromatograms, a tentative identification is possible with help of the absorption spectra recorded by the PDA detector and molecular formulas provided by the HRMS. Table S1 lists the most prominent BrC chromophores, along with their RTs, UV-vis absorption spectra, and provisional molecular formulas.^{33,46,47,66–69} Below, we discuss the elemental composition and plausible molecular structures of compounds corresponding to the 25 major light absorption peaks denoted in Figure 3a.

Peaks #1–12 are common BrC chromophores detected in the ESI– mode consistent with multiple previous reports.^{31,33,44,66} They are mainly CHON and CHO molecules. The CHON compounds contain 1 nitrogen atom and 4 oxygen atoms and can only be detected with ESI– mode, suggesting that they are nitrophenol derivatives. The UV–vis spectra of these compounds contain characteristic peaks making it possible to suggest plausible structures. For example, the BrC chromophore eluting at RT = 15.9–16.4 min (peak #4 in Table S1 and Figure 3a) correlates to a single MS peak with neutral elemental composition of C₆H₅NO₄, and its corresponding UV–vis spectrum exhibits a $\lambda_{\text{max}} \approx 345$ nm and a shoulder $\lambda \approx 309$ nm, resembling the UV–vis spectrum of 4-nitrocatechol (4NC).^{66,70} Similarly, chromophores #7 and #8 correspond to compounds C₈H₉NO₅ and C₇H₇NO₄, respectively. Their UV–vis spectra agree well with those of 4-nitrosyringol (4NS) and 4-nitroguaiacol (4NG), respectively.⁷¹ 4NC has been previously detected as an important BrC chromophore in fresh BB smoke particles as well as in ambient aerosols during the dry season of the Amazon rainforest and cloud droplets impacted by BB emissions.^{32,66} 4NS and 4NG have been previously detected in aged BBOA samples collected during a nationwide bonfire event in Israel.^{33,72} A variety of substituted phenols are typically produced from the pyrolysis of lignin during BB.^{73,74} These phenolic compounds can further react with NO₂ and NO₃ in the plume to form nitrophenols.⁷⁵ Nitrophenols have been previously used as tracer compounds for biomass burning secondary organic aerosol.⁷⁶ The results of this and previous studies^{44,48} suggest that nitrophenols are produced abundantly and quickly during common biomass burning events, which offers a highly oxidizing environment and releases a large amount of heat and reactive nitrogen species.⁷⁷ A recent study demonstrated that NO_x emissions from a flaming fire is 10–20 times higher than those from a smoldering fire.³⁸ Consequently, more nitroaromatic compounds were detected in BBOA from flaming burns, which also resulted in generally higher imaginary refractive indices for BrC light absorption than that from the smoldering fire.³⁸

Another type of BrC chromophores (e.g., #1, #3, and #5) detected in ESI– mode are CHO molecules characterized with high O/C ratios (>0.3). Despite the 100 min long chromatogram, these compounds are not well separated. Each PDA peak usually correlates with multiple CHO compounds eluting at the same time. Thus, it is difficult to determine their molecular structures based on a comparative analysis of their UV–vis and HRMS spectra. More detailed structural information for these compounds may be obtained using tandem mass spectrometry, which was not employed in this work. The tentative structures of these CHO compounds are proposed on the basis of the structures of plant tissue materials such as lignin and the molecular markers of BBOA reported in the literature.³⁹ These CHO compounds are relatively small aromatic compounds with 8–11 carbon atoms and multiple acidic polar functional groups, which allows them to elute earlier from the reversed-phase C18 column and be susceptible to ionization in the ESI– mode.

Peaks #14–17 represent typical chromophores observed in the ESI+ mode. Their UV–vis spectra exhibit fairly complex features characterized by multiple local absorption maxima, implying that each of the HPLC-PDA peaks correspond to either multiple coeluting chromophores or a single compound with a complex conjugation system. Two classes of compounds

are responsible for light absorption by these chromophores: CHO and CHN. The CHO compounds are characterized by low O/C ratios (<0.1) and high AI values (≥ 0.67), indicating that they are likely either oxygenated or O-heterocyclic PAHs (O-PAHs). The CHN compounds usually contain more than 17 carbon atoms and 1 to 2 nitrogen atoms, with AI > 0.67, suggesting they are likely N-heterocyclic PAHs (N-PAHs) with 4 to 6 aromatic rings fused together. CHN compounds are abundant in smoke particles produced by agricultural waste burning and forest fires.^{78–80} They are also abundant in cook stove emissions relying on dung for fuel.⁸¹ The large proton affinity of N-PAHs makes these compounds readily ionizable in ESI+ mode. It is suggested that smoldering fire can generate a large number of small N-heterocyclic compounds with 1 or 2 aromatic rings, mainly through thermal breakdown of N-bearing fragments of vegetation biofuels.⁸² At flaming stage, the higher burning temperature leads to pyrolysis of these CHN compounds as well as the N-containing plant materials producing additional N-PAHs.⁴⁴ Sage brush burning investigated in this study is dominated by flaming combustion, as evidenced by a high modified combustion efficiency (MCE = 0.95), which is an indicator of the relative contributions of flaming (namely, CO₂) and smoldering combustion (indicated by CO) phases averaged throughout the burning event.⁸³ The PDA chromatogram (Figure 3a) and UV–vis spectra (Table S1) of O- and N-PAHs suggest that they are important BrC chromophores absorbing significantly in the visible range (>400 nm) of solar radiation. Of note, although 1- or 2-ring N-heterocyclic compounds do not contribute substantially to BrC light absorption due to their insufficient number of conjugated double bonds, such basic N-heterocyclic compounds may serve as precursors of secondary BrC formed after their atmospheric aging.^{84–86}

Peaks #18–25 represent BrC chromophores that eluted last (RT > 55 min) from the C18 column, indicating they have strong hydrophobic properties. Compounds eluted during this period contain only carbon and hydrogen atoms in their formulas. These hydrocarbons usually contain at least 18 carbons and have high AI values (>0.67), suggesting they are PAHs with 4 to 9 condensed aromatic rings. They are readily ionized in the APPI mode and yield higher signals in APPI+ than in APPI–, which is in agreement with the results observed in direct infusion APPI-HRMS analysis (Figure 1b). Because O-PAHs and N-PAHs were observed at earlier RTs and found to contribute substantially to BrC light absorption, it is reasonable to expect that similar unsubstituted PAHs also should be abundant in this mixture. Both substituted and unsubstituted PAHs have similar formation mechanisms in the BB processes, which have been reported as the most important source of PAHs in the atmosphere.^{39,87} However, to date, the contribution of PAHs to the BrC light absorption has not been systematically evaluated.⁴⁹

Quantitative determination of the concentration of individual BrC chromophores based on the HPLC-MS measurement is a time-consuming task because it requires running chromatograms for multiple standards. Quantification without standards is not possible because compounds with different molecular structures have different and poorly predicted ionization efficiency in each of the modes. Previously, a few studies^{30,31,48} used authentic standards or surrogate compounds to calibrate the ionization efficiency and quantify the absolute mass concentration of several BrC chromophores. However, usually only a limited number of standard

compounds are available for such purpose. For instance, a recent study quantified eight nitroaromatics as BrC chromophores in ambient aerosols collected at different locations of Europe and China but only accounted for less than 0.2% of overall WSOC mass and 1–3% of the BrC light absorption at 370 nm.³⁰ Because of the large number of observed BrC chromophores, using standard compounds for quantitation was impractical and therefore was not attempted in this study.

Relative contributions of different classes of BrC chromophores to the overall solvent-extractable light absorption can be evaluated by combining the results from the HPLC-PDA and HPLC-HRMS chromatograms. According to the results illustrated by Figure 3 and Table S1, BrC chromophores in sage brush BBOA can be classified into five main categories depending on their elemental composition and polarity as described next. Polar BrC chromophores elute earlier from the HPLC column and are detected mainly by the ESI[−] mode. They are subdivided into two categories, polar CHO compounds and nitroaromatics, according to whether they have nitrogen in the elemental formula. As it is shown in Table S1, polar CHO compounds are mainly aromatics substituted with multiple polar functionalities including carboxyl, carbonyl, and hydroxyl groups. Aromatic acids and phenols are representative BrC chromophores in this category, while nitrophenols are typical BrC chromophores in the nitroaromatics category. The nonpolar fraction of BrC is mainly composed of PAHs with 4–9 fused rings, which elute very late from the column and are observed in both APPI modes. Compounds with RTs in between correspond to the semipolar fraction, in which O-PAHs and N-PAHs are the most typical BrC chromophores. The relative contribution of these classes of compounds to the overall solvent-extractable BrC light absorption is summarized in Figure 4. It is shown that over

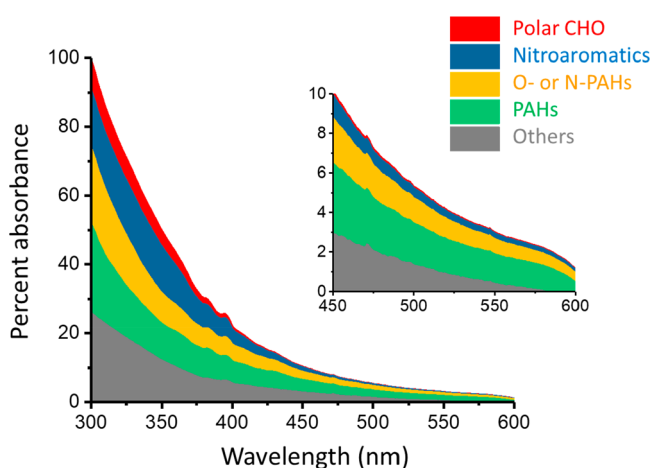


Figure 4. Contributions of different chromophore fractions to the overall solvent extractable BrC light absorption.

40% of the solvent-extractable BrC absorption in our selected sagebrush BBOA sample can be attributed to nonpolar and semipolar compounds such as PAHs and their derivatives (O-PAHs and N-PAHs). Polar CHO compounds and nitroaromatics collectively account for about 30% of the total absorption by the solvent-extractable BBOA. The remaining ~20% of the absorption could be attributed to a myriad of unresolved chromophores with either lower concentration or smaller molar absorption coefficient and possibly to charge

transfer complexes formed between internal segments of large molecules of BBOA.^{88,89}

CONCLUSION

Our results indicate that BrC chromophores in BBOA contain compounds with diverse molecular structures spanning a very broad range of molecular weights and polarities. The substantial differences between the BrC chromophores detectable by four different modes of ionization (APPI and ESI in positive and negative modes) result from inherent selectivity of the ionization processes. Using combined data obtained from different ionization modes, we were able to substantially expand the range of BrC compounds amenable to HRMS analysis. Subsequent analysis of species separated by HPLC and characterized by PDA and ESI/APPI-HRMS provided a better closure for the attribution of the observed absorption by the solvent-extractable BrC to specific chromophores. Specifically, for the BrC material presented in this study (BBOA emitted from test burns of sage brush biofuel), our results demonstrated that over 40% of the solvent-extractable BrC light absorption is contributed by nonpolar to semipolar compounds, such as PAHs and their derivatives, which could not be previously detected by ESI-based methods. The water-soluble BrC, such as nitroaromatics, phenols, and aromatic acids, account for less than 30% of the overall light absorption. Since the water insoluble fraction of BrC chromophores may contribute significantly to the overall BrC light absorption, future work is warranted to investigate their roles in regulating the chemical and physical processing of BrC in the atmosphere. The remaining 30% of the overall light absorption was attributed to collective effects of unresolved BrC chromophores.

Atmospheric brown carbon (BrC) is a complex organic mixture with its chemical characterization and environmental impacts poorly quantified yet. Since the majority of components in the BrC mixture are unknown, quantifying the concentration of individual components and evaluating their optical properties is impractical, yet tracking their dynamic evolution in the atmosphere is also challenging. In this paper, for the first time, we have demonstrated an analytical method which utilize ESI/APPI-HRMS as a qualitative probe for molecular level characterization and UV-vis spectroscopy (PDA detector) as a quantitative measure of light absorption capabilities to atmospheric BrC. With the combination of optimal HPLC separation, this method can provide both molecular identities to different types of organic compounds and evaluations of their contributions to light absorption. This method will be applied to investigate different BrC mixtures in future studies and significantly improve our understanding on the climate-relevant effects of atmospheric organic aerosols.

ASSOCIATED CONTENT

Supporting Information

The Supporting Information is available free of charge on the ACS Publications website at DOI: 10.1021/acs.analchem.8b02177.

UV-vis spectra of BrC extracted with three different solvents (Figure S1); list of formulas and UV-vis spectra of 25 major BrC chromophores detected by HPLC-PDA-HRMS analysis (Table S1) (PDF)

List of assigned formulas detected by direct infusion ESI/APPI-HRMS analysis (Appendix S1) (XLSX)

AUTHOR INFORMATION

Corresponding Author

*E-mail: alaskin@purdue.edu

ORCID

Sergey A. Nizkorodov: 0000-0003-0891-0052

Julia Laskin: 0000-0002-4533-9644

Alexander Laskin: 0000-0002-7836-8417

Notes

The authors declare no competing financial interest.

ACKNOWLEDGMENTS

We acknowledge support by the U.S. Department of Commerce, National Oceanic and Atmospheric Administration through Climate Program Office's AC4 program, awards NA16OAR4310101 and NA16OAR4310102. The HPLC-PDA-ESI/APPI-HRMS measurements were performed at the Environmental Molecular Sciences Laboratory (EMSL), a national scientific user facility located at PNNL, and sponsored by the Office of Biological and Environmental Research of the U.S. DOE.

REFERENCES

- (1) Schultz, M. G.; Heil, A.; Hoelzemann, J. J.; Spessa, A.; Thonicke, K.; Goldammer, J. G.; Held, A. C.; Pereira, J. M. C.; van het Bolscher, M. *Global Biogeochem. Cycles* **2008**, *22*, GB2002.
- (2) Sun, Y. L.; Jiang, Q.; Xu, Y. S.; Ma, Y.; Zhang, Y. J.; Liu, X. G.; Li, W. J.; Wang, F.; Li, J.; Wang, P. C.; Li, Z. Q. *J. Geophys. Res.: Atmos.* **2016**, *121*, 2508–2521.
- (3) Valerio, F. *Epidemiologia & Prevenzione* **2012**, *36*, 16–26.
- (4) Bougiatioti, A.; Bezantakos, S.; Stavroulas, I.; Kalivitis, N.; Kokkalis, P.; Biskos, G.; Mihalopoulos, N.; Papayannis, A.; Nenes, A. *Atmos. Chem. Phys.* **2016**, *16*, 7389–7409.
- (5) Jacobson, M. Z. *Journal of Geophysical Research-Atmospheres* **2014**, *119*, 8980–9002.
- (6) Reid, J. S.; Eck, T. F.; Christopher, S. A.; Koppmann, R.; Dubovik, O.; Eleuterio, D. P.; Holben, B. N.; Reid, E. A.; Zhang, J. *Atmos. Chem. Phys.* **2005**, *5*, 827–849.
- (7) Chen, J. M.; Li, C. L.; Ristovski, Z.; Milic, A.; Gu, Y. T.; Islam, M. S.; Wang, S. X.; Hao, J. M.; Zhang, H. F.; He, C. R.; Guo, H.; Fu, H. B.; Miljevic, B.; Morawska, L.; Thai, P.; Lam, Y. F.; Pereira, G.; Ding, A. J.; Huang, X.; Dumka, U. C. *Sci. Total Environ.* **2017**, *579*, 1000–1034.
- (8) Bond, T. C.; Zarzycki, C.; Flanner, M. G.; Koch, D. M. *Atmos. Chem. Phys.* **2011**, *11*, 1505–1525.
- (9) Chung, C. E.; Ramanathan, V.; Decremier, D. *Proc. Natl. Acad. Sci. U. S. A.* **2012**, *109*, 11624–11629.
- (10) Wang, X.; Heald, C. L.; Ridley, D. A.; Schwarz, J. P.; Spackman, J. R.; Perring, A. E.; Coe, H.; Liu, D.; Clarke, A. D. *Atmos. Chem. Phys.* **2014**, *14*, 10989–11010.
- (11) Saleh, R.; Marks, M.; Heo, J.; Adams, P. J.; Donahue, N. M.; Robinson, A. L. *Journal of Geophysical Research-Atmospheres* **2015**, *120*, 10285–10296.
- (12) Andreae, M. O.; Gelencser, A. *Atmos. Chem. Phys.* **2006**, *6*, 3131–3148.
- (13) Feng, Y.; Ramanathan, V.; Kotamarthi, V. R. *Atmos. Chem. Phys.* **2013**, *13*, 8607–8621.
- (14) Laskin, A.; Laskin, J.; Nizkorodov, S. A. *Chem. Rev.* **2015**, *115*, 4335–4382.
- (15) Moise, T.; Flores, J. M.; Rudich, Y. *Chem. Rev.* **2015**, *115*, 4400–4439.
- (16) Goldstein, A. H.; Galbally, I. E. *Environ. Sci. Technol.* **2007**, *41*, 1514–1521.
- (17) Lambe, A. T.; Cappa, C. D.; Massoli, P.; Onasch, T. B.; Forestieri, S. D.; Martin, A. T.; Cummings, M. J.; Croasdale, D. R.; Brune, W. H.; Worsnop, D. R.; Davidovits, P. *Environ. Sci. Technol.* **2013**, *47*, 6349–6357.
- (18) Sareen, N.; Moussa, S. G.; McNeill, V. F. *J. Phys. Chem. A* **2013**, *117*, 2987–2996.
- (19) Lee, H. J.; Aiona, P. K.; Laskin, A.; Laskin, J.; Nizkorodov, S. A. *Environ. Sci. Technol.* **2014**, *48*, 10217–10226.
- (20) Zhao, R.; Lee, A. K. Y.; Huang, L.; Li, X.; Yang, F.; Abbatt, J. P. D. *Atmos. Chem. Phys.* **2015**, *15*, 6087–6100.
- (21) Rincon, A. G.; Guzman, M. I.; Hoffmann, M. R.; Colussi, A. J. *J. Phys. Chem. Lett.* **2010**, *1*, 368–373.
- (22) De Haan, D. O.; Hawkins, L. N.; Kononenko, J. A.; Turley, J. J.; Corrigan, A. L.; Tolbert, M. A.; Jimenez, J. L. *Environ. Sci. Technol.* **2011**, *45*, 984–991.
- (23) Lee, A. K. Y.; Zhao, R.; Li, R.; Liggi, J.; Li, S. M.; Abbatt, J. P. D. *Environ. Sci. Technol.* **2013**, *47*, 12819–12826.
- (24) Nguyen, T. B.; Lee, P. B.; Updyke, K. M.; Bones, D. L.; Laskin, J.; Laskin, A.; Nizkorodov, S. A. *J. Geophys. Res.-Atmos* **2012**, *117*, D01207.
- (25) Turro, N. J.; Ramamurthy, V.; Scaiano, J. C. *Modern Molecular Photochemistry of Organic Molecules*; University Science Books: Sausalito, CA, 2010.
- (26) Bond, T. C.; Bergstrom, R. W. *Aerosol Sci. Technol.* **2006**, *40*, 27–67.
- (27) Hecobian, A.; Zhang, X.; Zheng, M.; Frank, N.; Edgerton, E. S.; Weber, R. J. *Atmos. Chem. Phys.* **2010**, *10*, 5965–5977.
- (28) Zhang, X. L.; Lin, Y. H.; Surratt, J. D.; Zotter, P.; Prevot, A. S. H.; Weber, R. J. *Geophys. Res. Lett.* **2011**, *38*, L21810.
- (29) Mohr, C.; Lopez-Hilfiker, F. D.; Zotter, P.; Prevot, A. S. H.; Xu, L.; Ng, N. L.; Herndon, S. C.; Williams, L. R.; Franklin, J. P.; Zahniser, M. S.; Worsnop, D. R.; Knighton, W. B.; Aiken, A. C.; Gorkowski, K. J.; Dubey, M. K.; Allan, J. D.; Thornton, J. A. *Environ. Sci. Technol.* **2013**, *47*, 6316–6324.
- (30) Teich, M.; van Pinxteren, D.; Wang, M.; Kecorius, S.; Wang, Z.; Müller, T.; Močnik, G.; Herrmann, H. *Atmos. Chem. Phys.* **2017**, *17*, 1653–1672.
- (31) Zhang, X. L.; Lin, Y. H.; Surratt, J. D.; Weber, R. J. *Environ. Sci. Technol.* **2013**, *47*, 3685–3693.
- (32) Desyaterik, Y.; Sun, Y.; Shen, X. H.; Lee, T. Y.; Wang, X. F.; Wang, T.; Collett, J. L. *Journal of Geophysical Research-Atmospheres* **2013**, *118*, 7389–7399.
- (33) Lin, P.; Bluvshstein, N.; Rudich, Y.; Nizkorodov, S. A.; Laskin, J.; Laskin, A. *Environ. Sci. Technol.* **2017**, *51*, 11561–11570.
- (34) Cheng, Y.; He, K.-b.; Du, Z.-y.; Engling, G.; Liu, J.-m.; Ma, Y.-l.; Zheng, M.; Weber, R. J. *Atmos. Environ.* **2016**, *127*, 355–364.
- (35) Liu, J.; Bergin, M.; Guo, H.; King, L.; Kotra, N.; Edgerton, E.; Weber, R. J. *Atmos. Chem. Phys.* **2013**, *13*, 12389–12404.
- (36) Xie, M. J.; Hays, M. D.; Holder, A. L. *Sci. Rep.* **2017**, *7*, 7318.
- (37) Chen, Y.; Bond, T. C. *Atmos. Chem. Phys.* **2010**, *10*, 1773–1787.
- (38) Sengupta, D.; Samburova, V.; bhattacharai, C.; Kirillova, E.; Mazzoleni, L.; Iankea-Lum, M.; Watts, A. C.; Moosmuller, H.; Khlystov, A. *Atmos. Chem. Phys. Discuss.* **2018**, aCP-2018-161.
- (39) Simoneit, B. R. T. *Appl. Geochem.* **2002**, *17*, 129–162.
- (40) Zhang, Y. P.; Williams, B. J.; Goldstein, A. H.; Docherty, K. S.; Jimenez, J. L. *Atmos. Meas. Tech.* **2016**, *9*, 5637–5653.
- (41) Zavahir, J. S.; Nolvachai, Y.; Marriott, P. J. *TrAC, Trends Anal. Chem.* **2018**, *99*, 47–65.
- (42) Lagesson-Andrasko, L.; Lagesson, V.; Andrasko, J. *Anal. Chem.* **1998**, *70*, 819–826.
- (43) Schug, K. A.; Sawicki, I.; Carlton, D. D.; Fan, H.; McNair, H. M.; Nimmo, J. P.; Kroll, P.; Smuts, J.; Walsh, P.; Harrison, D. *Anal. Chem.* **2014**, *86*, 8329–8335.
- (44) Lin, P.; Aiona, P. K.; Li, Y.; Shiraiwa, M.; Laskin, J.; Nizkorodov, S. A.; Laskin, A. *Environ. Sci. Technol.* **2016**, *50*, 11815–11824.
- (45) Lin, P.; Laskin, J.; Nizkorodov, S. A.; Laskin, A. *Environ. Sci. Technol.* **2015**, *49*, 14257–14266.

- (46) Lin, P.; Liu, J. M.; Shilling, J. E.; Kathmann, S. M.; Laskin, J.; Laskin, A. *Phys. Chem. Chem. Phys.* **2015**, *17*, 23312–23325.
- (47) Kitanovski, Z.; Grgic, I.; Vermeylen, R.; Claeys, M.; Maenhaut, W. *Journal of Chromatography A* **2012**, *1268*, 35–43.
- (48) Budisulistiorini, S. H.; Riva, M.; Williams, M.; Chen, J.; Itoh, M.; Surratt, J. D.; Kuwata, M. *Environ. Sci. Technol.* **2017**, *51*, 4415–4423.
- (49) Samburova, V.; Connolly, J.; Gyawali, M.; Yatavelli, R. L. N.; Watts, A. C.; Chakrabarty, R. K.; Zielinska, B.; Moosmuller, H.; Khlystov, A. *Sci. Total Environ.* **2016**, *568*, 391–401.
- (50) Cai, S.-S.; Syage, J. A.; Hanold, K. A.; Balogh, M. P. *Anal. Chem.* **2009**, *81*, 2123–2128.
- (51) Ghislain, T.; Faure, P.; Michels, R. *J. Am. Soc. Mass Spectrom.* **2012**, *23*, 530–536.
- (52) Jiang, B.; Liang, Y. M.; Xu, C. M.; Zhang, J. Y.; Hu, M.; Shi, Q. *Environ. Sci. Technol.* **2014**, *48*, 4716–4723.
- (53) Hockaday, W. C.; Purcell, J. M.; Marshall, A. G.; Baldock, J. A.; Hatcher, P. G. *Limnol. Oceanogr.: Methods* **2009**, *7*, 81–95.
- (54) Selimovic, V.; Yokelson, R. J.; Warneke, C.; Roberts, J. M.; de Gouw, J.; Reardon, J.; Griffith, D. W. T. *Atmos. Chem. Phys. Discuss.* **2017**, *2017*, 1–34.
- (55) Smith, D. R.; Robb, D. B.; Blades, M. W. *J. Am. Soc. Mass Spectrom.* **2009**, *20*, 73–79.
- (56) Pluskal, T.; Castillo, S.; Villar-Briones, A.; Oresic, M. *BMC Bioinf.* **2010**, *11*, 395–405.
- (57) Roach, P. J.; Laskin, J.; Laskin, A. *Anal. Chem.* **2011**, *83*, 4924–4929.
- (58) Eckert, P. A.; Roach, P. J.; Laskin, A.; Laskin, J. *Anal. Chem.* **2012**, *84*, 1517–1525.
- (59) Koch, B. P.; Dittmar, T. *Rapid Commun. Mass Spectrom.* **2006**, *20*, 926–932.
- (60) Koch, B. P.; Dittmar, T. *Rapid Commun. Mass Spectrom.* **2016**, *30*, 250–250.
- (61) Luosujarvi, L.; Arvola, V.; Haapala, M.; Pol, J.; Saarela, V.; Franssila, S.; Kotiaho, T.; Kostianen, R.; Kauppila, T. *Anal. Chem.* **2008**, *80*, 7460–7466.
- (62) Siegmann, K.; Sattler, K. *J. Chem. Phys.* **2000**, *112*, 698–709.
- (63) Lobodin, V. V.; Marshall, A. G.; Hsu, C. S. *Anal. Chem.* **2012**, *84*, 3410–3416.
- (64) Lung, S.-C. C.; Liu, C.-H. *Sci. Rep.* **2015**, *5*, 12992.
- (65) Kauppila, T. J.; Kotiaho, T.; Kostianen, R.; Bruins, A. P. *J. Am. Soc. Mass Spectrom.* **2004**, *15*, 203–211.
- (66) Claeys, M.; Vermeylen, R.; Yasmeen, F.; Gomez-Gonzalez, Y.; Chi, X. G.; Maenhaut, W.; Meszaros, T.; Salma, I. *Environmental Chemistry* **2012**, *9*, 273–284.
- (67) Friedel, R. A.; Orchin, M. *Ultraviolet spectra of aromatic compounds*; John Wiley & Sons, Inc.: New York, 1951.
- (68) Kitanovski, Z.; Cusak, A.; Grgic, I.; Claeys, M. *Atmos. Meas. Tech.* **2014**, *7*, 2457–2470.
- (69) Xie, M. J.; Chen, X.; Hays, M. D.; Lewandowski, M.; Offenber, J.; Kleindienst, T. E.; Holder, A. L. *Environ. Sci. Technol.* **2017**, *51*, 11607–11616.
- (70) Cornard, J. P.; Rasmiwetti, Merlin, J. C. *Chem. Phys.* **2005**, *309*, 239–249.
- (71) Tang, H.; Thompson, J. E. *Open J. Air Pollut.* **2012**, *1*, 22746.
- (72) Bluvshstein, N.; Lin, P.; Flores, J. M.; Segev, L.; Mazar, Y.; Tas, E.; Snider, G.; Weagle, C.; Brown, S. S.; Laskin, A.; Rudich, Y. *Journal of Geophysical Research: Atmospheres* **2017**, *122*, 5441–5456.
- (73) Mazzoleni, L. R.; Zielinska, B.; Moosmuller, H. *Environ. Sci. Technol.* **2007**, *41*, 2115–2122.
- (74) Simoneit, B. R. T.; Rogge, W. F.; Mazurek, M. A.; Standley, L. J.; Hildemann, L. M.; Cass, G. R. *Environ. Sci. Technol.* **1993**, *27*, 2533–2541.
- (75) Harrison, M. A. J.; Barra, S.; Borghesi, D.; Vione, D.; Arsene, C.; Olariu, R. L. *Atmos. Environ.* **2005**, *39*, 231–248.
- (76) Iinuma, Y.; Boge, O.; Grafe, R.; Herrmann, H. *Environ. Sci. Technol.* **2010**, *44*, 8453–8459.
- (77) Benedict, K. B.; Prenni, A. J.; Carrico, C. M.; Sullivan, A. P.; Schichtel, B. A.; Collett, J. L. *Atmos. Environ.* **2017**, *148*, 8–15.
- (78) Laskin, A.; Smith, J. S.; Laskin, J. *Environ. Sci. Technol.* **2009**, *43*, 3764–3771.
- (79) Lin, P.; Rincon, A. G.; Kalberer, M.; Yu, J. Z. *Environ. Sci. Technol.* **2012**, *46*, 7454–7462.
- (80) Wang, Y. J.; Hu, M.; Lin, P.; Guo, Q. F.; Wu, Z. J.; Li, M. R.; Zeng, L. M.; Song, Y.; Zeng, L. W.; Wu, Y. S.; Guo, S.; Huang, X. F.; He, L. Y. *Environ. Sci. Technol.* **2017**, *51*, 5951–5961.
- (81) Fleming, L. T.; Lin, P.; Laskin, A.; Laskin, J.; Weltman, R.; Edwards, R. D.; Arora, N. K.; Yadav, A.; Meinardi, S.; Blake, D. R.; Pillarisetti, A.; Smith, K. R.; Nizkorodov, S. A. *Atmos. Chem. Phys.* **2018**, *18*, 2461–2480.
- (82) Ma, Y. L.; Hays, M. D. *Journal of Chromatography A* **2008**, *1200*, 228–234.
- (83) Jolleys, M. D.; Coe, H.; McFiggans, G.; McMeeking, G. R.; Lee, T.; Kreidenweis, S. M.; Collett, J. L.; Sullivan, A. P. *J. Geophys. Res. Atmos.* **2014**, *119*, 12850–12871.
- (84) Montoya-Aguilera, J.; Horne, J. R.; Hinks, M. L.; Fleming, L. T.; Perraud, V.; Lin, P.; Laskin, A.; Laskin, J.; Dabdub, D.; Nizkorodov, S. A. *Atmos. Chem. Phys.* **2017**, *17*, 11605–11621.
- (85) Aiona, P. K.; Lee, H. J.; Lin, P.; Heller, F.; Laskin, A.; Laskin, J.; Nizkorodov, S. A. *Environ. Sci. Technol.* **2017**, *51*, 11048–11056.
- (86) Romonosky, D. E.; Ali, N. N.; Saiduddin, M. N.; Wu, M.; Lee, H. J.; Aiona, P. K.; Nizkorodov, S. A. *Atmos. Environ.* **2016**, *130*, 172–179.
- (87) Lu, H.; Zhu, L. Z.; Zhu, N. *Atmos. Environ.* **2009**, *43*, 978–983.
- (88) Phillips, S. M.; Smith, G. D. *Environ. Sci. Technol. Lett.* **2014**, *1*, 382–386.
- (89) Phillips, S. M.; Smith, G. D. *J. Phys. Chem. A* **2015**, *119*, 4545–4551.